Preprints.org

Article

Microwave Field Characteristics of Nitrogen-Vacancy Centers in Diamond for Living Cell Temperature Measurement

Zhen Xian Fan , Li Xing [*] , Fei Xiang Wu , Xiao Juan Feng [*] , Jin Tao Zhang

Article

Microwave Field Characteristics of Nitrogen-Vacancy Centers in Diamond for Living Cell Temperature Measurement

Zhenxian Fan [1,2], Li Xing [2,*], Feixiang Wu [3], Xiaojuan Feng [2,*] and Jintao Zhang

[1]   Department of Precision Instrument, Tsinghua University, Beijing 100084, China
[2]   National Institute of Metrology, Beijing 100029, China
[3]   College of Mechanical and Electrical Engineering, China Jiliang University, Hangzhou 310018, China
*   Correspondence: xingli@nim.ac.cn (L.X.); fengxj@nim.ac.cn (X.F.)

Abstract: A typical solid-state quantum sensor can be developed based on negatively charged nitrogen-vacancy (NV$^-$) centers in diamond. The electron spin state of NV$^-$ can be controlled and read at room temperature. Through optical detection magnetic resonance (ODMR) technology, temperature measurement inside living cells can be achieved at the nanoscale. The key to ODMR technology is to apply microwave resonance to manipulate the electron spin state of NV$^-$. Therefore, the microwave field characteristics formed near the NV$^-$ have a crucial impact on the sensitivity of ODMR measurement. This article mainly focuses on the temperature situation in cellular applications, and simulates the influence of structural parameters of double open loop resonant (DOLR) microwave antennas and broadband large-area (BLA) microwave antennas on the microwave field's resonance frequency, quality factor Q, magnetic field strength, uniformity, etc. The parameters are optimized to have sufficient bandwidth, high signal-to-noise ratio, low power loss, and high magnetic field strength in the temperature range of 36 ℃ to 42.5 ℃. Finally, the ODMR spectra are used for effect comparison, and the signal-to-noise ratio and Q values of the ODMR spectra are compared when using different antennas. We have provided an optimization method for the design of microwave antennas and it is concluded that the DOLR microwave antenna is more suitable for living cell temperature measurement in our study.

Keywords: NV$^-$centers in diamond; microwave field characteristics; microwave antenna; living cell temperature measurement

1. Introduction

Temperature is a fundamental factor reflecting the physical and chemical changes in living organisms. For example, living cells can cause internal temperature changes when responding to environmental changes [1,2], but the temperature changes generated by this process are usually small and brief [3], posing a challenge to temperature measurement technology. In recent years, existing intracellular temperature measurement technologies, such as fluorescent proteins [4], organic dyes [5], and rare earth particles [6], generally suffer from low measurement accuracy [7], insufficient temporal and spatial resolution, and unstable fluorescence [8]. The method of NV centers in diamond stand out due to its stable physical and chemical properties, good biocompatibility [9,10], ultra-high sensitivity in electronic spin measurement [11]. Meanwhile it can measure multiple physical quantities such as temperature [12–14], magnetic field [15,16], pressure [17,18], electric field [19,20], etc. Therefore, it has become an emerging micro nano-scale quantum measurement technology, especially in the fields of temperature and magnetic measurement. In 2010, the principle of temperature measurement was first proposed by D. Budker et al. [21] and the sensitivity of zero field splitting energy D to temperature was discovered. In 2021, the sensitivity was reached the level of $76\,\mu K/\sqrt{Hz}$ [7]. The NV centers sensing technology requires microwave tuning, and the microwave field characteristics will directly affect the measurement signal-to-noise ratio. Microwave fields can

be generated through different types of microwave antennas, among which the microwave field generated by straight copper wire antennas has poor uniformity, and the field strength decreases rapidly with increasing distance from the wire. The microwave field strength generated by a circular antenna is more uniform, but the field strength is often much weaker than that of a single copper wire [22]. For a resonator antenna, the shape, size, and thickness of the surface copper will determine the resonance frequency and magnetic field uniformity.

Therefore, in recent years, domestic and foreign research groups have designed various microwave antennas to meet the different requirements of NV center thermometers applied in different scenarios. In 2014, K. Bayat et al. designed a double open loop resonant (DOLR) microwave antenna with a resonance frequency near 2.87 GHz at room temperature. The antenna has a good quality factor, narrow bandwidth, and is suitable for ODMR spectral line measurement with a single resonant peak [23]. In 2015, D. S. Rudnicki et al. designed a microwave antenna that can adjust the resonance frequency between 2.7 GHz and 3.1 GHz, corresponding to a magnetic field of 0-100 Gauss, allowing the microwave to be arbitrarily adjusted between linear polarization and circular polarization. However, the distance between micro-strip lines must match the distance between the micro-strip line and the excitation point in order to obtain a good polarization state, resulting in strong position dependence and high calibration difficulty [24]. In 2016, K. Sasaki et al. designed a microwave antenna that operates near 2.87 GHz at room temperature, with a bandwidth of around 400 MHz. It can directly apply to observe multiple Zeeman level splitting peaks under an external magnetic field, without readjusting the antenna's resonance frequency [22]. After 2018, researches on antennas mainly focus on optimizing uniformity in three-dimensional space. Among them, Tang Jun's team [25] designed a large-area three-dimensional uniform microwave antenna, which can increase the bandwidth and improve the contrast of ODMR. Multiple resonance frequencies can be manipulated and kept the antenna away from the sample without interfering with the objective lens or sample by increasing the signal-to-noise ratio (SNR) of the antenna. Moreover, the impact of microwave heating on diamond can be suppressed and quality factors can be improved. In the same year, Chu-Feng Liu's team [7] designed a dielectric resonator antenna for three-dimensional uniform operation of NV centers, achieving a Rabi frequency of 10 MHz in 7 mm^3 space, which can increase the sensitivity of magnetometers by two orders of magnitude.

At present, the design of microwave antennas is mainly aimed at applications at room temperature or situations with external magnetic fields. However, there is a lack of further analysis on antennas used in cellular environments. On the basis of existing antenna design, this article conducts parameter optimization design research to meet the requirements of microwave field in cell experiments. In recent years, the electromagnetic properties at the cells and molecules have also received attention with the deepening of interdisciplinary research. The configuration of culture dishes [26], dielectric parameters, and electromagnetic parameters of culture media can all affect the microwave field characteristics, thereby affecting the temperature measurement of NV centers. The temperature range of the cell activity research is 36 ℃~42.5 ℃, that is, from the optimal culture temperature for live cells to the temperature at which tumor cell are killed. The corresponding frequencies of zero field splitting energy are about 2.86892 GHz~2.86844 GHz. The microwave antenna itself has a more significant thermal effect, comparing with the relatively small changes in the thermal environment of cells. Thus, the influence of microwave thermal effect needs to be considered, and it was first observed in the study of Fujiwara et al. [27]. However, it only qualitatively revealed the existence of this phenomenon and its impact on temperature measurement accuracy. Quantitative research can be found in Ref. [28], which showed that the temperature rise caused by microwave thermal effect increases with the increase of the application time and power. At a microwave power of 6 dBm, the maximum temperature rise can reach 43.68 K. The temperature difference that living cells can adapt to is only about 5.5 K. The heat generated by microwaves is transferred to cells through the culture medium, which not only affects the accuracy of temperature measurement but also causes cell death. In summary, the requirements for microwave field characteristics in living cell temperature measurement mainly include: 1. High *Q* value and low heat

production; 2. Low return loss and high energy transmission efficiency of microwave antennas; 3. Bandwidth and magnetic field uniformity meet requirements, but not demanding.

This article conducts in-depth research on the microwave characteristics of two types of irregular microwave antennas, double open loop resonance (DOLR) and broadband and large-area (BLA) microwave antenna, in the temperature measurement of living cell. Firstly, the characteristics of microwave field required for cell temperature measurement has been analyzed. Secondly, the characteristics of antenna microwave $S11$ parameters, magnetic field strength and uniformity, as well as quality factor have been simulated, and parameter optimization methods were studied. Finally, ODMR spectral line tests were conducted to compare performance of the straight copper wire (SCW) antenna and the optimized irregular antenna. The improvement of microwave field characteristics was verified through changes in spectral line contrast, line width, and signal-to-noise ratio.

2. The fundamental principles

Diamond crystal is a tetrahedron composed of carbon atoms, each of which forms a covalent bond with the other four carbon atoms in a sp³ hybrid orbital, exhibiting high symmetry [29]. When one of the carbon atoms is replaced by a nitrogen atom and the adjacent carbon atom is replaced by a vacancy, a nitrogen vacancy center is formed. According to whether it is negatively charged or not, the nitrogen vacancy centers can be divided into two types: NV⁰ and NV⁻, which can be converted to each other under certain environmental conditions [30,31]. The outermost layer of NV⁻ has two free electrons that can generate zero field splitting through spin-spin interaction. The zero-field splitting energy D is temperature dependent, so temperature measurement can be achieved through spin manipulation.

As shown in Figure 1, the ground state of the NV center includes $m_s = \pm 1$ and $m_s = 0$. The zero-field splitting D of the ground state electronic spins at room temperature is about 2.87 GHz. ODMR spectral lines can be obtained by scanning the microwave frequency and collecting the fluorescence [32–34]. When the NV color center is excited from the ground state to the excited state, there are two ways of de-excitation. One is spontaneous emission transition, which mainly occurs in the electronic spins in the excited state of $|0>$. The electronic spins in this process directly returns from the excited state to the ground state and radiates photons. Another type is Intersystem Crossing (ISC), which mainly occurs when the electronic spins is in the excited state of $|\pm 1>$. This process reaches a metastable state before returning to the ground state without radiating photons. From the perspective of fluorescence brightness, $|0>$ is in the bright state and $|\pm 1>$ is in the dark state. The function of microwaves is to manipulate the electronic spins between the $|0>$ state and the $|\pm 1>$ state, causing population flipping. When the microwave frequency is the same as the frequency of zero field splitting energy D, the population of electronic spins in the $|\pm 1>$ state is the highest, resulting in the lowest fluorescence emitted by the NV⁻. Moreover, the variation of microwave power can cause a change in the population of electron spin in the $|\pm 1>$ state, manifested as a variety in ODMR contrast. In addition, changes in microwave power can cause changes in the spectral line width [27]. The contrast C and line width Δv directly affect the theoretical signal-to-noise ratio of temperature measurement $\eta_T(K/\sqrt{Hz})$, i.e $\eta_T(K/\sqrt{Hz}) \approx P_F \left(\frac{dT}{dv}\right)_{T_0} \Delta v/(C\sqrt{R})$. It can be known that the larger the contrast C and the narrower the line width Δv, the higher the signal-to-noise ratio. Therefore, the design of microwave antennas is crucial.
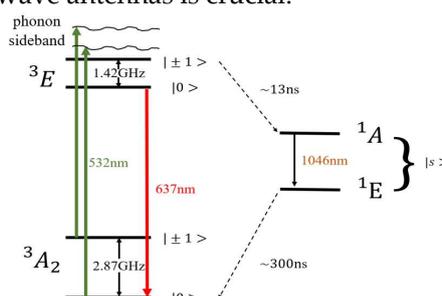
Figure 1. The energy level structure of NV⁻ center without considering external magnetic field and stress.

The DOLR and BLA microwave antenna studied by K. Bayat [23] and K. Sasaki [22] are suitable for room temperature applications, as shown in Figure 2. The impact of culture dishes and media on the performance of microwave antennas in cell temperature measurement was not considered. Therefore, it is necessary to optimize the structural parameters to make them suitable for cell research scenarios.
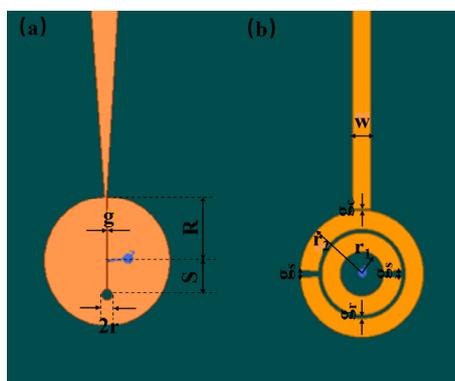

Figure 2. Schematic diagram of two types of irregular microwave antennas. (**a**) BLA microwave antenna structure; (**b**) DOLR microwave antenna structure.

3. Simulation and optimization of irregular antennas

3.1. Microwave radiation element simulation

Firstly, numerical simulation was conducted based on the microwave antenna structural parameters set in K. Bayat [23] and K. Sasaki [22]'s paper. The simulation results are analyzed from the aspects of $S11$ parameters, quality factor Q, magnetic field strength, uniformity, etc.

For the center frequency of microwave antennas, the BLA microwave antennas is 2.9680 GHz, which is 0.098 GHz larger than 2.87 GHz with a frequency deviation of about 3.4%. The center frequency of the DOLR microwave antenna is 2.8797 GHz, which is close to the microwave frequency corresponding to zero field splitting energy in room temperature, with only a frequency deviation of 0.3%. The center frequency of the two type antennas can be adjusted later by pasting copper strips. The bandwidth of BLA microwave antennas can reach 400 MHz, ensuring that Zeeman level splitting lines can be observed under an external magnetic field of up to 100 Gauss. For DOLR microwave antennas, its bandwidth is only a few tens of megahertz, making it difficult to measure multiple resonance peaks simultaneously within the bandwidth range. However, for the temperature measurement of cell environmental, the D value changes by about 400 kHz, and the bandwidth requirement is not strict. The S11 parameters of the two antennas are shown in Figure 3. The return loss of the DOLR microwave antenna is relatively smaller, thus the power transmission efficiency of the DOLR microwave antenna is higher. The quality factor Q is the ratio of the electromagnetic energy stored in the resonator to the energy lost in one cycle, which is related to the ohmic loss of the metal wire, the dielectric loss of the printed circuit board, the radiation loss, and the coupling loss of the microstrip line. Its value can be obtained by the ratio of center frequency to line width. The larger the Q, the less thermal effect is generated by microwave loss, but the bandwidth will also be correspondingly decreased. The microwave field characteristics of the two antennas are listed in Table 1, and the quality factor of the DOLR microwave antenna is relatively higher than that of BLA antenna. In summary, the DOLR microwave antenna is more suitable for situations where the antenna heating effects need to be weakened and measured at the nanoscale.
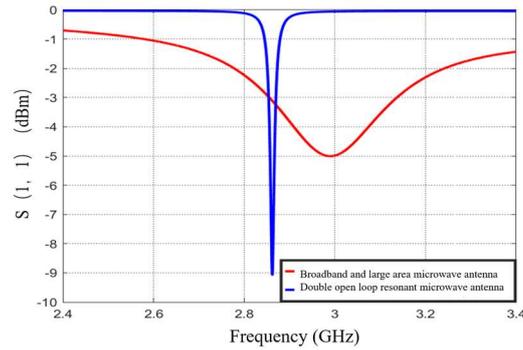
Figure 3. S11 spectra of two types of microwave antennas.

Table 1. Microwave Field Characteristics of Microwave Antennas.

Antenna type / Microwave field characteristics	BLA microwave antenna	DOLR microwave antenna
Center frequency (GHz)	2.968	2.880
Bandwidth (MHz)	379	19
Q value	7.8	151.6
Uniformity of Microwave Field on Different Areas of Microwave Antennas ($H'_{\text{homogeneity}} = (H_{\max} - H_{\min})/H_{\text{mid}}$)	4 mm*4 mm	4 mm*4 mm
	1.945	1.799
	3 mm*3 mm	3 mm*3 mm
	1.893	1.746
	2 mm*2 mm	2 mm*2 mm
	1.796	1.266
	1 mm*1 mm	1 mm*1 mm
	0.774	0.654
Radiation element microwave field strength $H_{\max}$ (A/m)	4405.7236	2569.4648
Considering the microwave field strength under the diamond chip model $H'_{\max}$(A/m)	82.8191	36.6272

The simulations of microwave field strength in the radiation element region are shown in Figure 4. For BLA microwave antennas, the overall field strength distribution decreases outward from the center of a small circular notch with a microwave element radius of r (Figure 2), and is symmetrically distributed along the gap g (Figure 2). Therefore, diamond samples should be placed at the center of the small circular notch, and the microwave field strength in the radiation element region at the sample placement is shown in Figure 5a, with a maximum field strength of 82.8191 A/m. For the double open loop resonant microwave antenna as shown in Figure 4b, it is symmetrical along the x-axis at the center (the x-axis and y-axis are in the diamond horizontal plane, and the z-axis is perpendicular to the plane), decreasing along the z-axis. Therefore, the sample should be placed at the center of the antenna, and the field strength near the sample placement is shown in Figure 5b, with a maximum field strength of 36.6272 A/m. In terms of microwave field uniformity, we use $(H_{max} - H_{min})/H_{mid}$ to calculate the magnetic field uniformity $H'_{homogeneity}$, and the smaller the value, the better the surface uniformity. For the xy plane, as shown in Table 1, for BLA microwave antennas and DOLR microwave antennas, the smaller the area, the better the uniformity. When the area is within 1 mm², the uniformity is close to and less than 1, and the planar uniformity of the DOLR microwave antenna is slightly better. In addition, the microwave field strength within the range of 0-10 mm from the antenna surface in the z-axis direction has been analyzed. As shown in Figure 6, the field strength of both types of antennas shows a trend of first increasing and then decreasing with

increasing the distance, whose maximum points are located around 2 mm from the xy plane of the antenna. Therefore, the NV centers recommended to be placed at about 2 mm away from the surface of the antenna. Moreover, the diamond does not directly contact with the antenna, and the heating effect on the diamond is also reduced. Diamond can be placed on a 3D printed hollow brackets, or an optical tweezers can be used to control the position of the nanodiamonds to achieve this goal. In theory, considering the effects of return loss, thermal effects, magnetic field strength, etc., the DOLR antenna may be more suitable for applications in cellular environments.
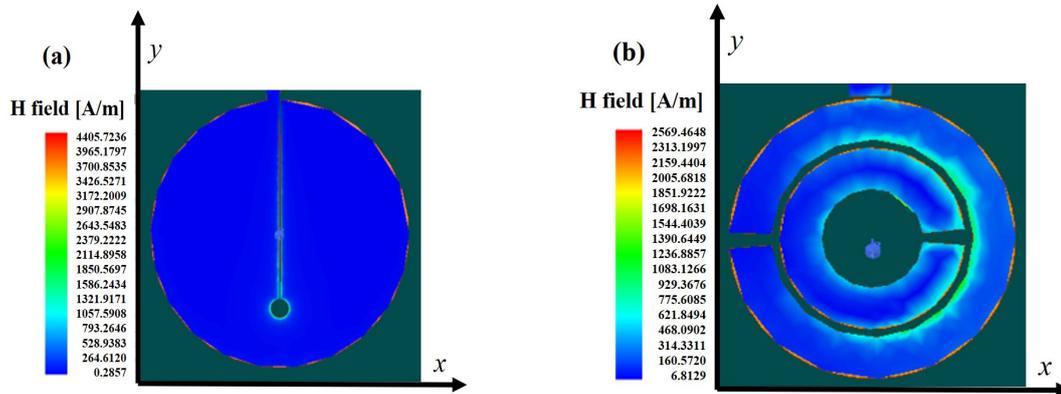

Figure 4. Simulation results of microwave field strength in the radiation element region. (**a**) BLA microwave antenna (H_{max}=4405.7236 A/m); (**b**) DOLR microwave antenna (H_{max}=2569.4648 A/m).
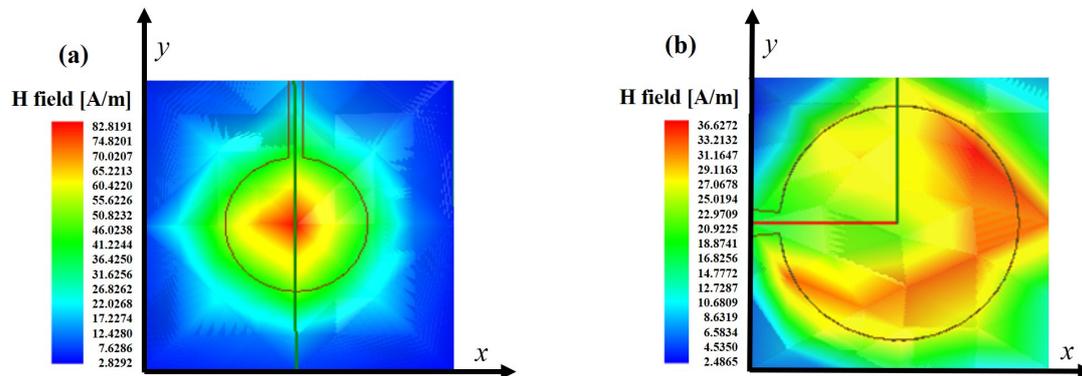

Figure 5. Simulation results of microwave field strength in the radiation element area where diamond samples are placed. (**a**) BLA microwave antenna (H_{max}=82.8191 A/m); (**b**) DOLR microwave antenna (H_{max}=36.6272 A/m).
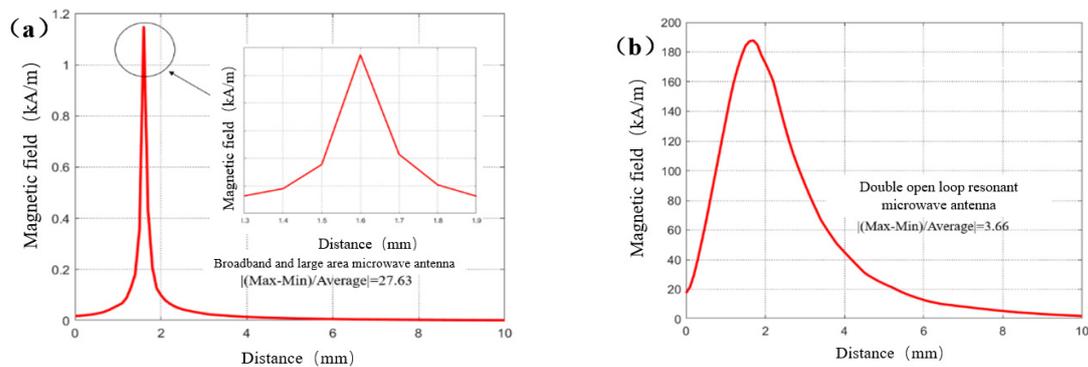

Figure 6. Simulation results of magnetic field strength along z-axis. (**a**) BLA microwave antenna diagram; (**b**) DOLR microwave antenna.

3.2. Model optimization

In recent years, many people have been studying the *D-T* relationship of the NV centers thermometer [35]. For instance, a third-order polynomial has been proposed to fit the *D-T* relationship in the temperature range of 300 K-600 K [33]. The optimal temperature for human cell activity is known to be (36.5 ± 0.5) ℃. If the temperature inside the cell exceeds 42.5 ℃ or is irradiated for a long time at this temperature, the active cells, and even tumor cells, will be uniformly killed [36–39]. Therefore, we set the experimental study temperature at 36 ℃-42.5 ℃, at which $dD/dT \approx$-74.2 kHz/K, and the corresponding change in *D* value is about 400 kHz. In the cellular application scenario, diamond does not directly contact the microwave antenna but is swallowed by the cells. The simulations in Figure 6 show that the maximum field intensities of the two irregular antennas are about 2 mm away from the surface, so it has a natural advantage in this aspect. Both cells and diamonds are suspended in a solution environment, so that microwaves need to pass through the culture dish (dielectric constant ε_r=3.01, loss tangent angle tanδ=0.0015), glass slide (dielectric constant ε_r=5.42, loss tangent angle tanδ=0.044) and culture medium (conductivity σ=5400 ± 100 μs/cm) to act on the NV centers. The culture medium, culture dish, and glass slide will affect the center frequency and the heating effect of the microwave antenna. Water is the main component of the culture medium, with a higher specific heat capacity, making it easy to absorb the heat generated by the antenna. Therefore, it directly affects the environmental temperature and cell activity. In the design process, it is necessary to consider correcting the offset of the center frequency in advance, and focus on reducing the influence of thermal effects, that is, improving the quality factor *Q* and *S*11 parameters of the microwave antenna. In addition, media such as culture dishes and culture media can cause microwave power loss. On the premise of ensuring the accuracy of the center frequency and minimal heating effect, the microwave field strength should be increased as much as possible to improve the effectiveness of microwave power acting on cells. Based on the above analysis, we established a model in the cellular environment, as shown in Figure 7.
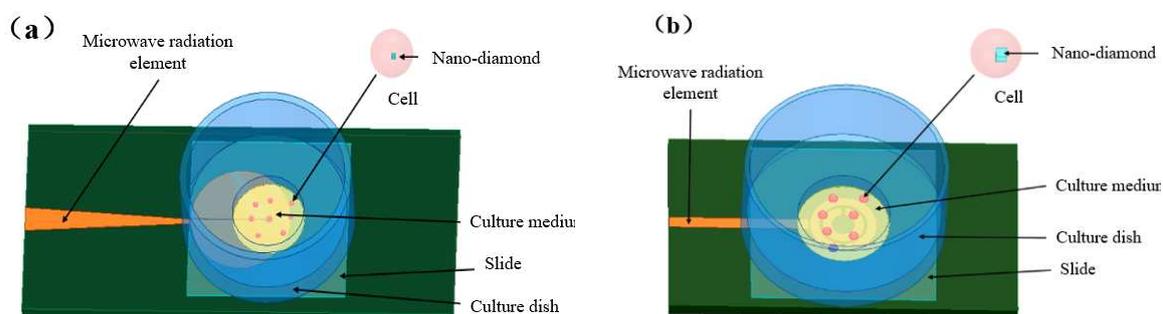

Figure 7. Model diagrams of two types of microwave antennas in a cellular environment. (**a**) Model diagram of the BLA microwave antenna; (**b**) Model diagram of the DOLR microwave antenna.

As shown in Figure 8, materials such as diamond samples and culture dishes will affect the microwave resonance frequency of the antenna, causing a left shift of the center frequency. Compared to the resonance frequency of the original design of the antenna in Table 2, sheet-like diamond only causes a frequency shift of 0.0105 GHz, while the cellular environment causes a frequency shift of 0.4009 GHz for BLA microwave antennas, which is 40 times greater than that in the case of sheet-like diamonds. For the DOLR microwave antenna, the sheet-like diamond causes a frequency shift of 0.0069 GHz, and the cellular environment causes a frequency shift of 0.1589 GHz, which is about 23 times more than that in the case of sheet-like diamonds. The DOLR antenna has a smaller offset than the BLA antennas. For the cellular environment, it is necessary to optimize the antenna size again based on the influence of culture dishes, culture media, and glass slides to reduce the center frequency offset. Moreover, the bandwidth of BLA antenna can reach 400 MHz, while the bandwidth of DOLR antenna is only about 20 MHz. It is known that the frequency variety of zero field splitting energy *D* caused by temperature changes in the cellular environment is about 400 kHz, so that both the two

antennas meet the bandwidth requirements. The heating effect of microwave antennas can be reflected by their quality factor Q value, where the larger the Q value, the smaller the heating effect. As shown in Table 2, the Q value of a BLA antenna is about 7 in different environments. The Q value of a DOLR microwave antenna is about 130 in a single radiation element and diamond sheet, which is about 18 times more than that of BLA antenna. The Q value is about 32 in a cellular environment, which is 4.6 times more than that that of BLA antenna. Therefore, the heating effect of BLA antenna is larger. Both types of antennas have the highest Q value under the condition of pure radiation element without medium. The Q value of the DOLR antenna significantly decreases in the cellular environment, while that of BLA remains almost unchanged.
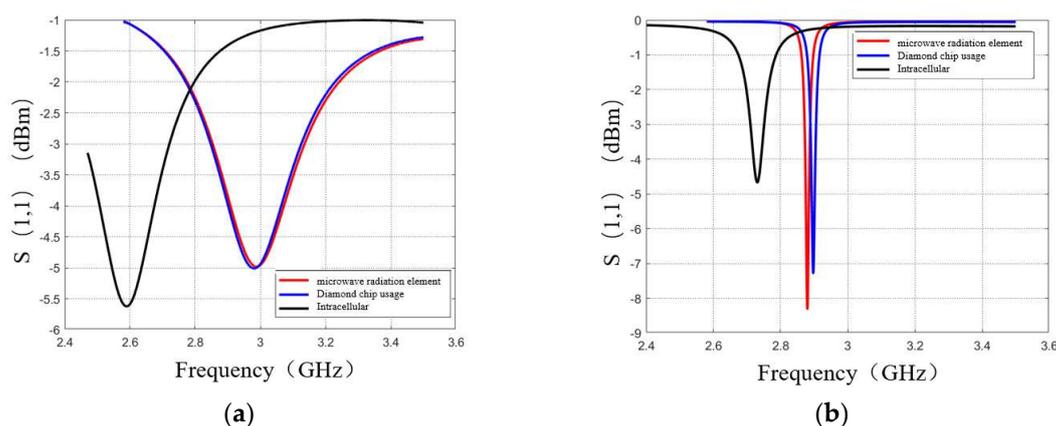

Figure 8. S11 parameters of the two microwave antennas under different environmental conditions. (**a**) S11 parameters of BLA microwave antenna in different environments; (**b**) S11 parameters of DOLR microwave antenna in different environments.

In terms of magnetic field strength, as shown in Table 2, it can be seen that BLA microwave antennas have a greater advantage in magnetic field strength for diamond sheets, which can still reach over 2000 A/m. However, it drops sharply to 236.9 A/m in cellular application environments. The DOLR microwave antenna is less than 1000 A/m in all the three environments. In the cellular environment, the magnetic field strength of DOLR antenna is only about 70 A/m less than that of BLA antenna. In terms of magnetic field uniformity, the diamond sheet environment is analyzed based on a 4 mm * 4 mm region. The uniformity of the DOLR and BLA antennas is 1.975 and 1.882, respectively. The case of cellular environment is analyzed based on a 1 mm * 1 mm region. The uniformity of the DOLR and BLA antennas is 0.424 and 0.958, respectively. Thus, the uniformity of the DOLR antenna is better than that of the BLA antenna.

In summary, for the application scenarios of diamond sheets, the advantages of BLA antenna lie in their wide bandwidth and strong magnetic field strength. The advantages of DOLR antenna are low heat loss, high signal-to-noise ratio Q value, and good magnetic field uniformity. For cellular application, the design of high Q value and low heat loss are required, and DOLR antenna are more suitable for this situation. In addition, it can be concluded that the impact of culture dishes, culture media, and other factors on the antenna in cellular application is significantly different from that of diamond sheets. Thus, it is necessary to optimize the size of the irregular antennas to make its microwave field characteristics such as center frequency, heat loss, and magnetic field uniformity more in line with the needs of cellular application.

For cellular application scenarios, the requirements for the center frequency offset, magnetic field uniformity, and heating effects of the microwave field generated by the antenna are different from the diamond sheets. The optimization conditions are determined as follows: the center frequency is around 2.87 GHz to achieve the conditions of NV centers resonance. Heat loss depletion and return loss should be minimized as much as possible, that is, the Q value and S11 parameter should be as large as possible, in order to reduce the impact of heat loss on temperature measurement accuracy and cell activity. Furthermore, the magnetic field uniformity may be improved under the

premise of meeting the previous requirements, to reduce the impact of NV centers' position on measurement accuracy.

Table 2. The microwave field characteristics of two types of microwave antennas in different environments.

Antenna type / Microwave field characteristics		BLA microwave antenna	DOLR microwave antenna
Center frequency (GHz)	Radiation element	2.9902	2.8902
	Diamond sheet	2.9797	2.8971
	Cellular environment	2.5893	2.7313
Bandwidth (MHz)	Radiation element	381.8	19.5
	Diamond sheet	421.5	22.3
	Cellular environment	336.7	83.6
Q value	Radiation element	7.83	148.2
	Diamond sheet	7.07	130.00
	Cellular environment	7.69	32.7
Magnetic field strength (A/m)	Radiation element	2366.5	948.5
	Diamond sheet	2871.5	413.00
	Cellular environment	236.9	161.4
Magnetic field uniformity	Radiation element	1.999	1.933
	Diamond sheet	1.975	1.882
	Cellular environment	0.958	0.424

The optimization design of the DOLR antenna is carried out in Figure 9. The original dimensions (as shown in Figure 2b) are as follows. The radii of inner and outer rings are r_1=1.2 mm, r_2=2.4 mm and the ring width is $d=r_2-r_1$=1.2 mm. The coupling gap is g_c=0.05 mm, and the gap at the crack is g_s=0.4 mm. The gap between the two rings is g_r=0.2 mm, and the lead width is w =1 mm. Based on the above dimensions, a univariate control method is adopted to simulate the effects of different dimensions on the center frequency and bandwidth. In Figure 9, it can be seen that when the coupling gap g_c is 0.04 mm, both the center frequency and bandwidth can be maximized simultaneously. When the gap between the two rings g_r is 0.2 mm, the center frequency is the highest but the bandwidth is reduced by 20 MHz. When g_r is 0.15 mm, the bandwidth is maximum, but the center frequency is offset by about 0.1 GHz, which is relatively larger compared to the bandwidth offset of diamond itself. The requirement of bandwidth is not high, so priority is given to meeting the center frequency requirement of the ODMR spectral lines. Therefore, a gap g_r of 0.2 mm between the two rings is selected. The inner ring radius r_1 is optimized from 1.0 mm to 1.2 mm. The center frequency is closest to 2.87 GHz with a value of r_1=1.085 mm. When the lead width w is between 1.2 mm and 1.6 mm, the difference in center frequency and bandwidth is not significant. Considering reducing the thermal contact area and saving metal materials, it is decided to choose a lead width of 1.2 mm. Based on the simulation parameters of g_c=0.04 mm, g_r=0.2 mm, r_1=1.085 mm, w=1.2 mm, g_s=0.4 mm and d=1.2 mm, it was found that the center frequency would be larger than 2.87 GHz. Therefore, adjustments are made to r_1 and w in the direction of slightly reducing the center frequency. When the gap g_s is 0.45 mm, the center frequency is maximum, followed by 0.35 mm. In order to bring the center frequency back to around 2.87 GHz, g_s =0.35 mm is chosen. Based on the determination of the first five dimensions, the ring width d ($d=r_2-r_1$) is adjusted from 1.2 mm to 1.0 mm as shown in Figure 9f. As shown in Figure 10, the center frequency of the antenna is 2.8744 GHz, and the bandwidth is 71 MHz. The return loss S11 is -6.8 dBm at the center frequency, and the quality factor Q value is 40.43, which meets the requirements.
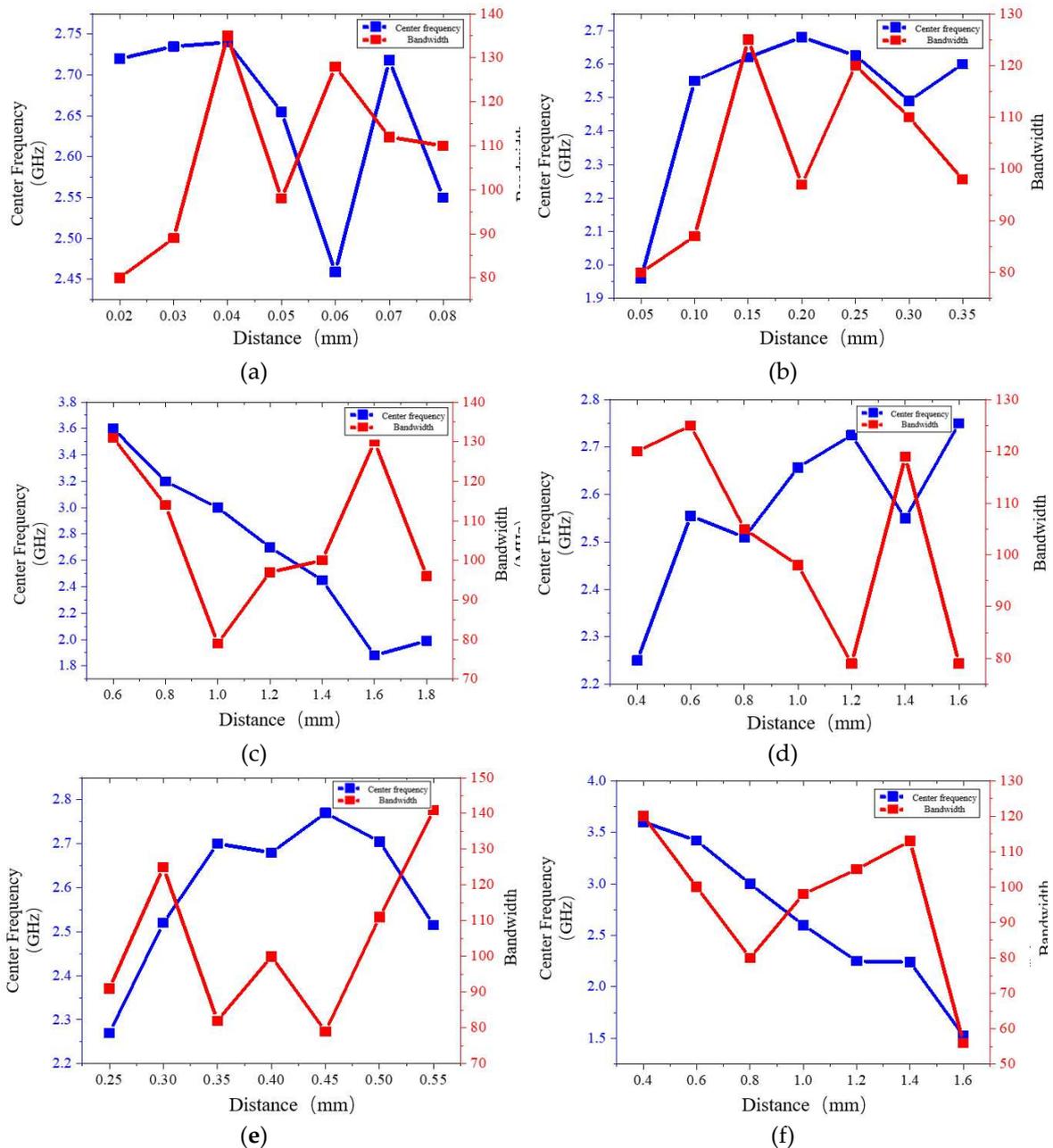
Figure 9. Diagram of the relationship between structural parameters and center frequency of DOLR microwave antennas in cellular application scenarios. (**a**) The relationship between coupling gap g_c and center frequency or bandwidth; (**b**) The relationship between the gap g_r and the center frequency or bandwidth; (**c**) The relationship between inner ring radius r_1 and center frequency or bandwidth; (**d**) The relationship between lead width w and center frequency or bandwidth; (**e**) The relationship between the gap g_s and the center frequency or bandwidth; (**f**) The relationship between ring width d and center frequency or bandwidth.

Similarly, for BLA microwave antenna, the parameter optimization process is shown in the Appendix A. After optimizing the center frequency and bandwidth, the following parameters are selected: r=0.20 mm, R=6.98 mm, g=0.2 mm, and S=3.9 mm. The results are shown in the blue line in Figure 10. At this time, the center frequency is 2.8715 GHz, and the bandwidth is about 311 MHz. The return loss $S11$ is -7 dBm at the center frequency, and the quality factor Q value is 9.22.
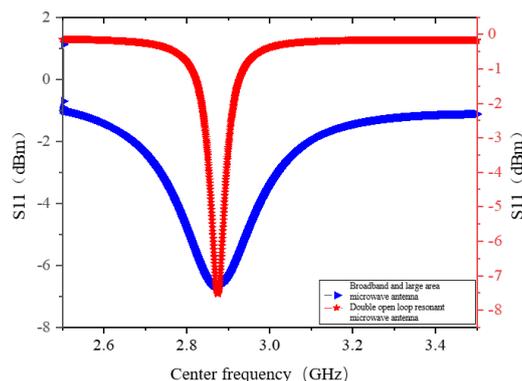
Figure 10. Optimization results of S-parameters for BLA microwave antennas (blue line) and DOLR microwave antennas (red line).

The optimization results of the above two microwave antennas have been analyzed for Q value, magnetic field uniformity, and magnetic field strength. As shown in Table 3, the Q value of the DOLR antenna is nearly three times that of the BLA antenna. Therefore, the DOLR antenna has smaller heating effect. In terms of planar magnetic field uniformity based on the analysis of 4 mm * 4 mm, the BLA antenna is 0.992 larger than the DOLR antenna. In terms of magnetic field strength, the DOLR antenna is nearly three times that of BLA microwave antenna. In summary, the DOLR antenna has higher signal-to-noise ratio, better magnetic field performance and smaller heat effect, making it more suitable for cell research experiments.

Table 3. Microwave field characteristics of optimized microwave antennas.

Antenna type	Q value	Uniformity of planar magnetic field	Magnetic field strength (A/m)
BLA microwave antenna	9.22	1.967	144.1
DOLR microwave antenna	40.43	0.975	344.9

4. ODMR experiments and Discussion

The experimental platform is shown in Figure 11. A continuous laser emitted by a 532 nm laser undergoes collimation and beam expansion after changing the direction of the optical path through planar reflectors. Then, it is incident onto an acousto-optic modulator (AOM) (AODR 1080AF-DIF0-1.0, Gooch&Housego, UK), which generates high-speed switching modulation of the laser. The laser enters the multimode fiber and focuses on the sample by the reflection of a dichroic mirror. The NV centers in diamond emit fluorescence ranging from 600 nm to 800 nm after laser excitation. It passes through a dichroic mirror and filters out the remaining reflected laser at 532 nm through a filter (FELH0600, Thorlabs, USA). Finally, the fluorescence is collected by a converging lens and incident onto a single photo counting module (SPCM). A data acquisition (DAQ) is used to process the number of photons collected by SPCM. Microwave is generated by a microwave source (SMIQ 06B, Rohde&Schwarz, USA), and then amplified by an amplifier (ZHL-16W-43-S+, Mini Circuits, USA) to a microwave antenna. The RF switch (ZASWA-2-50DRA+, Mini Circuits, USA) is applied to control the on/off of the microwave signal. The system uses a pulse generator (PBESR-PRO-500-PCI, SpinCore, USA) to achieve pulse control of microwave and laser.
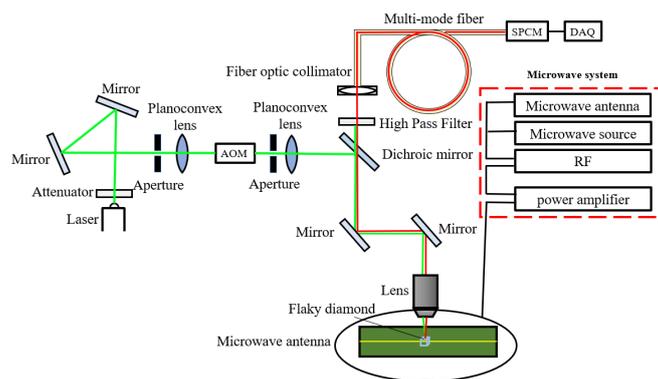
Figure 11. The diagram of ODMR experimental system.

The ODMR spectral lines of NV centers have been measured at -24 dBm, -20 dBm, -15 dBm, -10 dBm, and -5 dBm based on a straight wire antenna. The changes in contrast and bandwidth are observed as shown in Figure 12. With the increase of microwave power, both the contrast and bandwidth of the ODMR spectrum become larger. The value of zero-field splitting energy *D* shifted to the left, indicating an increase in microwave heating effect and thermal noise. As shown in Figure 13, using line bandwidth/contrast represents the signal-to-noise ratio (SNR) of spectral lines measurement. It can be seen that the smaller the value, the higher the SNR, and the higher the limit sensitivity level of the system measurement. As the microwave power increases, the SNR first increases and then decreases, indicating the existence of an optimal value. After the microwave power in this system exceeds -10 dBm, the SNR will slightly decrease due to the heating effect and thermal noise. Therefore, when the microwave power is set at -10 dBm, the SNR is optimal, and the heating effect and thermal noise are lower at this time.
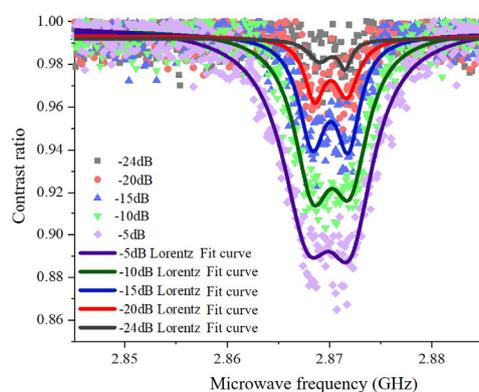

Figure 12. ODMR spectra at microwave fields of -5 dBm, -10 dBm, -15 dBm, -20 dBm, and -24 dBm based on a straight wire antenna.
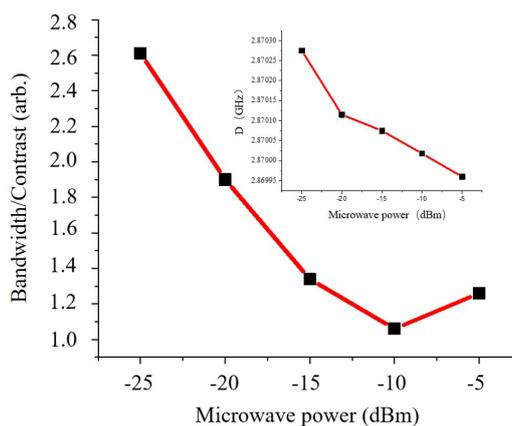
Figure 13. The variation of signal-to-noise ratio of a straight wire microwave antenna with microwave power.

As shown in Figure 14, the values of bandwidth/contrast for the three antennas have been compared. For DOLR microwave antennas, the SNR reaches its optimal value when the microwave power is around -10 dBm. The optimal microwave power of the straight wire microwave antenna is also around -10 dBm, but its SNR is lower than that of the DOLR microwave antenna. For BLA microwave antenna, the optimal microwave power is around -15 dBm. The SNR rapidly decreases above -15 dBm, and the SNR remains basically unchanged in the range of -25 dBm to -15 dBm. Its overall SNR is also lower than that of the DOLR antenna. In the range of -25 dBm to -16 dBm, the SNR of BLA antenna is better than that of straight wire antenna. In summary, within the power range of -25 dBm to-5 dBm, the DOLR antenna has the best ultimate sensitivity and signal-to-noise ratio.
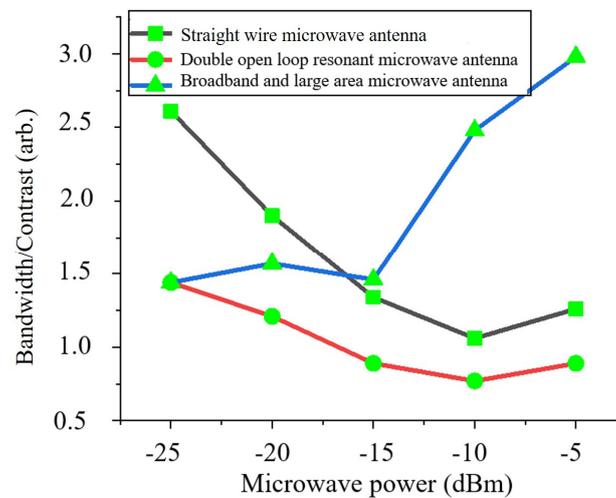

Figure 14. Comparison for SNR of the three types of microwave antennas.

It is also important to ensure the accuracy of temperature measurement while improving the signal-to-noise ratio. Therefore, the heating effect of the antenna itself is expected to be as small as possible, and the quality factor Q is increased. The quality factor Q of the three antennas can be calculated by the center frequency/bandwidth (full width at half height), as shown in Figure 15. It can be seen that the DOLR antenna is generally superior to the other two antennas. For the DOLR antenna, the Q value attenuation is not significant in the microwave power range of -25 dBm to -15 dBm. However, when the microwave power is greater than -15 dBm, the Q values will quickly decrease. Therefore, the DOLR antenna has the best SNR at -15 dBm with high quality factor and small heating effect. The Q values of the other two antennas show an approximately linear decreasing trend with increasing microwave power. When the microwave power is less than -15 dBm, the Q value of the BLA antenna is slightly better than that of the straight wire antenna. When the microwave power is greater than -15 dBm, the Q value of straight wire antenna is higher. Considering both of the heating effect and SNR, the DOLR microwave antenna is the optimal choice, and its microwave power can be optimized in the range of -15 dBm to -10 dBm.
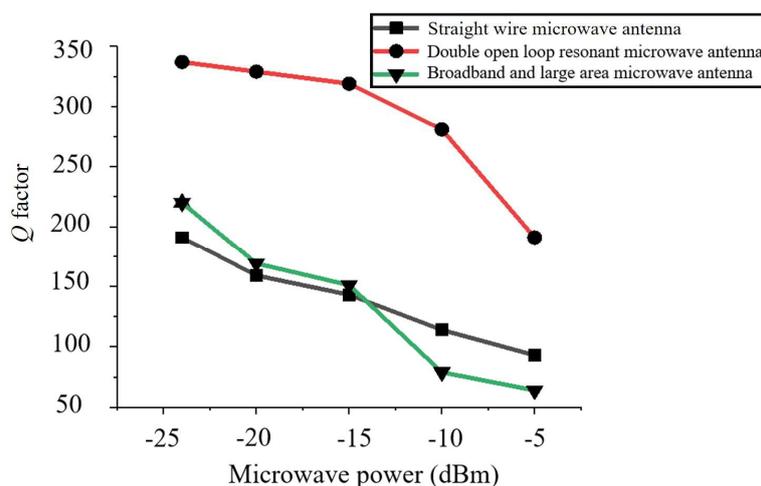
Figure 15. Comparison of Q values for the three types of microwave antennas.

5. Conclusions

This paper focuses on the application scenarios of cell temperature measurement, which require microwave antennas with high Q value, low return loss, and small heating effect. The comparative analysis was conducted on the characteristics of DOLR antenna and BLA microwave antenna. The advantages of BLA microwave antenna lie in their wide bandwidth and high magnetic field strength, but their obvious disadvantages lie in their large heating effect and return loss. The advantages of DOLR microwave antenna lie in their high Q value, small $S11$ parameter and the heating effect. Its magnetic field uniformity is good, so that the DOLR antenna is more suitable for cellular applications. Moreover, the influence of culture medium, culture dish, etc. on the center frequency, bandwidth, magnetic field properties, etc. of the microwave antennas have been analyzed. The structure parameters of the microwave antenna have been optimized to ensure that the center frequency and bandwidth of the antenna meet the requirements. On this basis, the Q value and magnetic field strength should be maximized as much as possible, and the heat loss and thermal effect should be minimized as much as possible. Finally, the signal-to-noise ratio and Q value of the straight wire antenna, DOLR antenna, and BLA antenna were quantified and compared through ODMR experiments. The advantages of DOLR microwave antennas in low heating effect and high SNR have been proved. Secondly, the trend of SNR and Q value with microwave power variation, as well as the optimal power value were obtained by power optimization. This article provides a simulation and verification method for designing and optimizing microwave antennas in special environments. Its partial requirements for antennas are also applicable to the magnetic field measurement of NV centers in diamond.
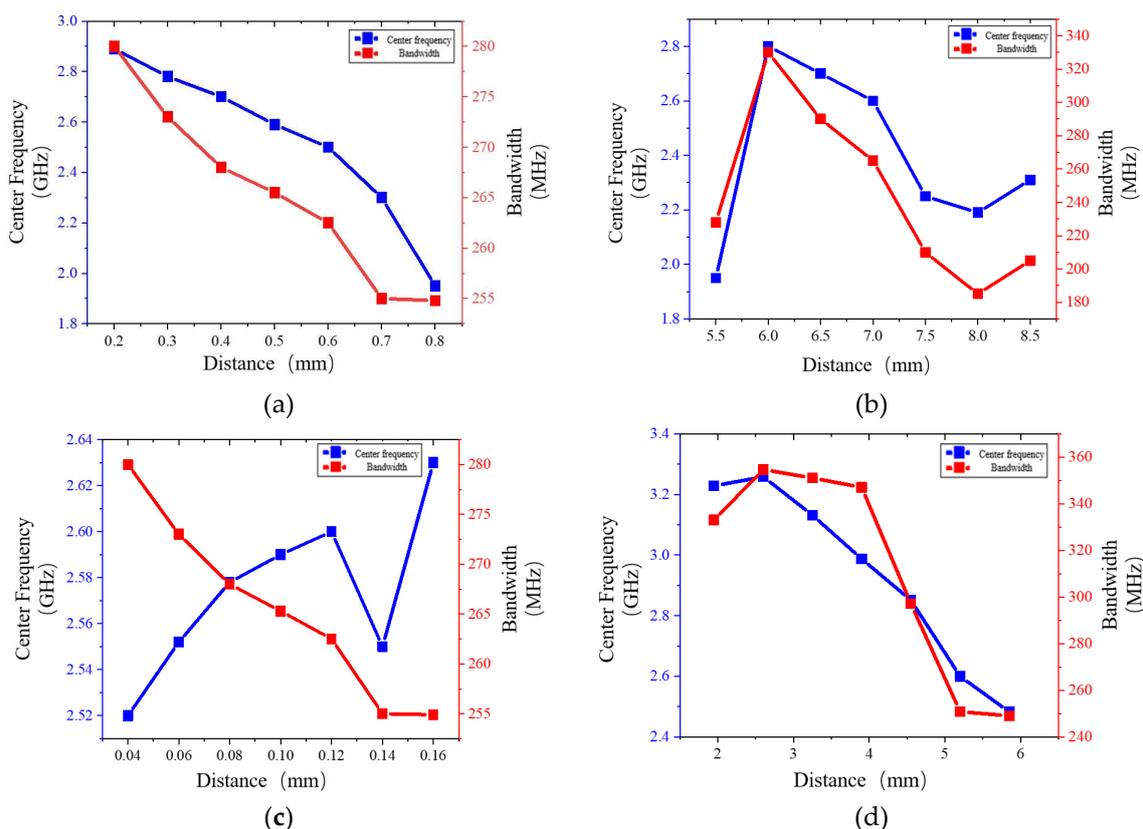
Appendix A

Figure A1. A. Simulation results of structural parameters optimization of BLA microwave antenna (**a**) The relationship between ring radius *r* and center frequency or bandwidth; (**b**) The relationship between hole radius *R* and center frequency or bandwidth; (**c**) The relationship between gap *g* and center frequency or bandwidth; (**d**) The relationship between the distance *S* and center frequency or bandwidth.

References

1. Seymour, R.S. Biophysics and Physiology of Temperature Regulation in Thermogenic Flowers. *Biosci. Rep.* **2001**, *21*, 223-236.
2. Patel, D.; Franklin, K.A. Temperature-regulation of plant architecture. *Plant. Signal. Behav.* **2009**, *4*, 577-579.
3. Fan, J.W.; Cojocaru, I.; Becker, J.; Fedotov, I.V.; Alkahtani, M.H.A.; Alajlan, A.; Blakley, S.; Rezaee, M.; Lyamkina, A.; Palyanov, Y.N.; Borzdov, Y.M.; Yang, Y.P.; Zheltikov, A.; Hemmer, P.; Akimov, A.V. Germanium-vacancy color center in diamond as a temperature sensor. *ACS Photonics.* **2018**, *5*, 765-770.
4. Donner, J.S.; Thompson, S.A.; Kreuzer, M.P.; Baffou, G.; Quidant, R. Mapping intracellular temperature using green fluorescent protein. *Nano Lett.* **2012**, *12*, 2107-2111.
5. Okabe, K.; Inada, N.; Gota, C.; Harada, Y.; Funatsu, T.; Uchiyama, S. Intracellular temperature mapping with a fluorescent polymeric thermometer and fluorescence lifetime imaging microscopy. *Nat. Commun.* **2012**, *3*, 705.
6. Ximendes, E.C.; Santos, W.Q.; Rocha, U.; Kagola, U.K.; Sanz-Rodríguez, F.; Fernández, N.; Gouveia-Neto, A.d.S.; Bravo, D.; Domingo, A.M.; Rosal, B.d.; Brites, C.D.S.; Carlos, L.D.; Jaque, D.; Jacinto, C. Unveiling in vivo subcutaneous thermal dynamics by infrared luminescent nanothermometers. *Nano Lett.* **2016**, *16*, 1695-1703.
7. Liu, C.F.; Leong, W.H.; Xia, K.; Feng, X.; Finkler, A.; Denisenko, A.; Wrachtrup, J.; Li, Q.; Liu, R.B. Ultrasensitive hybrid diamond nanothermometer. *NSR.* **2021**, *5*, nwaa194.
8. Bernardi, E.; Moreva, E.; Traina, P.; Petrini, G.; Tchernij, S.D.; Forneris, J.; Pastuović, Ž.; Degiovanni, I.P.; Olivero, P.; Genovese, M. A biocompatible technique for magnetic field sensing at (sub)cellular scale using nitrogen-vacancy centers. *EPJ Quantum Technolo.* **2020**, *7*,13.
9. Yu, S.J.; Kang, M.W.; Chang, H.C.; Chen, K.M.; Yu, Y.C. Bright fluorescent nanodiamonds: No photobleaching and low cytotoxicity. *JACS.* **2005**, *127*, 17604-17605.

10. Fu, C.C.; Lee, H.Y.;Chen, K.; Lim, T.S.; Wu, H.Y.; Lin, P.K.;Wei, P.K.; Tsao, P.H.; Chang, H.C.; Fann, W. Characterization and application of single fluorescent nanodiamonds as cellular biomarkers. *PNAS.* **2007**, *104*, 727-732.

11. Xie, Y.; Yu, H.; Zhu, Y.; Qin, X.; Rong, X.; Duan, C.K.; Du, J. A hybrid magnetometer towards femtotesla sensitivity under ambient conditions. *Sci. Bull.* **2021**, *66*, 127-132.

12. Neumann, P.; Jacobi, I.; Dolde, F.; Burk, C.; Reuter, R.; Waldherr, G.; Honert, J.;   Wolf, T.; Brunner, A.; Shim, J.H.; Suter, D.; Sumiya, H.; Isoya, J.; Wrachtrup, J. High-precision nanoscale temperature sensing using single defects in diamond. *Nano Lett.* **2013**, *13*, 2738-2742.

13. Toyli, D.M; de las Casas, C.F.; Christle, D.J.; Dobrovitski, V.V.; Awschalom, D.D.; Fluorescence thermometry enhanced by the quantum coherence of single spins in diamond. *PNAS.* **2013**, *110*, 8417-8421.

14. Plakhotnik, T.; Doherty, M.W.; Cole, J.H.; Chapman, R.; Manson, N.B. All-optical thermometry and thermal properties of the optically detected spin resonances of the NV⁻ Center in nanodiamond. *Nano Lett.* **2014**, *14*, 4989-4996.

15. Maze, J.R.; Stanwix, P.L.; Hodges, J.S.; Hong, S.; Taylor, J.M.; Cappellaro, P.; Jiang, L.; Gurudev Dutt, M.V.; Togan, E.; Zibrov, A.S.; Yacoby, A.; Walsworth, R.L.; Lukin, M.D. Nanoscale magnetic sensing with an individual electronic spin in diamond. *Nature.* **2008**, *455*, 644-647.

16. Taylor, J.M.; Cappellaro, P.; Childress, L.; Jiang, L.; Budker, D.; Hemmer, P.R.; Yacoby, A.; Walsworth, R.; Lukin, M.D. High-sensitivity diamond magnetometer with nanoscale resolution. *Nat. Phys.* **2008**, *4*, 810-816.

17. Ivády, V.; Simon, T.; Maze, J.R.; Abrikosov, I.A.; Gali, A. Pressure and temperature dependence of the zero-field splitting in the ground state of NV centers in diamond: A first-principles study. *PRB.* **2014**, *90*, 235205.

18. Doherty, M.W.; Struzhkin, V.V.; Simpson, D.A.; McGuinness, L.P.; Meng, Y.; Stacey, A.; Karle, T.J.; Hemley, R.J.; Manson, N.B.; Hollenberg, L.C.L.; Prawer, S. Electronic properties and metrology applications of the diamond NV− center under pressure. *PRL.* **2014**, *112*, 047601.

19. Dolde, F.; Fedder, H.; Doherty, M.W.; Nöbauer, T.; Rempp, F.; Balasubramanian, G.; Wolf, T.; Reinhard, F.; Hollenberg, L.C.L.; Jelezko, F.; Wrachtrup, J. Electric-field sensing using single diamond spins. *Nat. Phys.* **2011**, *7*, 459-463.

20. Iwasaki, T.; Naruki, W.; Tahara, K.; Makino, T.; Kato, H.; Ogura, M.; Takeuchi, D.; Yamasaki, S.; Hatano, M. Direct nanoscale sensing of the internal electric field in operating semiconductor devices using single electron spins. *ACS nano.* **2017**, *11*, 1238-1245.

21. Jensen, K.; Leefer, N.; Jarmola, A.; Dumeige, Y.; Acosta, V.M.; Kehayias, P.; Patton, B.; Budker, D. Cavity-enhanced room-temperature magnetometry using absorption by nitrogen-vacancy centers in diamond. *Phys. Rev. Lett.* **2014**, *112*, 160802.

22. Sasaki, K.; Monnai, Y.; Saijo, S.; Fujita, R.; Watanabe, H.; Ishi-Hayase, J.; Itoh, K.M.; Abe, E. Broadband, large-area microwave antenna for optically detected magnetic resonance of nitrogen-vacancy centers in diamond. *RSI.* **2016**, *87*.

23. Bayat, K.; Choy, J.; Farrokh Baroughi, M.; Meesala, S.; Loncar, M. Efficient, Uniform, and large area microwave magnetic coupling to NV centers in diamond using double split-ring resonators[J]. Nano Letters. 2014, 14, 1208-1213.

24. Kapitanova, P.; Soshenko, V.V.; Vorobyov, V.V.; Dobrykh, D.; Bolshedvorskii, S.V.; Sorokin, V.N.; Akimov, A.V. 3D uniform manipulation of NV centers in diamond using a dielectric resonator antenna. *JETP LETT+.* **2018**, *108*, 588-595.

25. Chen, Y.; Guo, H.; Li, W.; Wu, D.; Zhu, Q.; Zhao, B.; Wang, L.; Zhang, Y.; Zhao, R.; Liu, W.; Du, F.; Tang, J.; Liu, J. Large-area, tridimensional uniform microwave antenna for quantum sensing based on nitrogen-vacancy centers in diamond. *APEX.* **2018**, *11*, 123001.

26. Gao, Y.C.; Sun, J.H.; Yu, G.F. Measurement of dielectric constant of cell culture dishes. *Journal of University of Electronic Science and Technology of China.* **2007**, *36*, 70-72.

27. Fujiwara, M.; Sun, S.; Dohms, A.; Nishimura, Y.; Suto, K.; Takezawa, Y.; Oshimi, k.; Zhao, L.; Sadzak, N.; Umehara, Y.; Teki, Y.; Komatsu, N.; Benson, O.; Shikano, Y.; Kage-Nakadai, E. Real-time nanodiamond thermometry probing in vivo thermogenic responses. *Sci. Adv.* **2020**, *6*, eaba9636.

28. Wang, Z.; Zhang, J.T.; Feng, X.J.; Xing, L. Microwave heating effect on diamond samples of nitrogen-vacancy centers. *ACS Omega.* **2022**, *7*, 31538-31543.

29. Loubser, J.H.N.; van Wyk, J.A. Electron spin resonance in the study of diamond. *Rep. Prog. Phys.* **1978**, *41*, 1201.

30. Felton, S.; Edmonds, A.M.; Newton, M.E.; Martineau, P.M.; Fisher, D.; Twitchen, D.J.; Baker, J.M. Hyperfine interaction in the ground state of the negatively charged nitrogen vacancy center in diamond. *PRB.* **2009**, *79*, 075203.

31. Barry, J.F.; Turner, M.J.; Schloss, J.M.; Glenn, D.R.; Song, Y.; Lukin, M.D.; Park, H.; Walsworth, R.L. Optical magnetic detection of single-neuron action potentials using quantum defects in diamond. *PNAS.* **2016**, *113*, 14133-14138.

32. Schoenfeld, R.S.; Harneit, W. Real time magnetic field sensing and imaging using a single spin in diamond. *PRL.* **2011**, *106*, 030802.

33. Toyli, D.M.; Christle, D.J.; Alkauskas, A.; Buckley, B.B.; Van de Walle, C.G.; Awschalom, D.D. Measurement and control single nitrogen-vacancy center spins above 600K. *PRX.* **2012**, *2*, 031001.

34. Doughty, A.C.V.; Hoover, A.R.; Layton, E.; Murray, C.K.; Howard, E.W.; Chen, W. R. Nanomaterial applications in photothermal therapy for cancer. Materials. *Nat. Mater.* **2019**, 12, 779.

35. Acosta, V.M.; Bauch, E.; Ledbetter, M.P.; Waxman, A.; Bouchard, L.S.; Budker, D. Temperature dependence of the nitrogen-vacancy magnetic resonance in diamond. *PRL.* **2010**, *104*, 070801.

36. Hsiao, C.W.; Chuang, E.Y.; Chen, H.L.; Wan, D.; Korupalli, C.; Liao, Z.X.; Chiu, Y.L.; Chia, W.T.; Lin, K.J.; Sung, H.W. Photothermal tumor ablation in mice with repeated therapy sessions using NIR-absorbing micellar hydrogels formed in situ. *Biomaterials.* **2015**, *56*, 26−35.

37. Chen, Q.; Xu, L.; Liang, C.; Wang, C.; Peng, R.; Liu, Z. Photothermal therapy with immune-adjuvant nanoparticles together with checkpoint blockade for effective cancer immunotherapy. *Nat. Commun.* **2016**, *7*, 13193.

38. Zhang, C.; Bu, W.; Ni, D.; Zuo, C.; Cheng, C.; Li, Q.; Zhang, L.; Wang, Z.; Shi, J. A polyoxometalate cluster paradigm with self-adaptive electronic structure for acidity/reducibility-specific photothermal conversion. *JACS.* **2016**, *138*, 8156−8164.

39. Wu, Y.K.; Alam, M.N.A.; Balasubramanian, P.; Ermakova, A.; Fischer, S.; Barth, H.; Wagner, M.; Raabe, M.; Jelezko, F.; Weil, T. Nanodiamond theranostic for light-controlled intracellular heating and nanoscale temperature sensing. *Nano Lett.* **2021**, *21*, 3780−3788.